

SUPPLEMENTARY INFORMATION

Edge Contacts accelerate the Response of MoS₂ Photodetectors

Fabian Strauß^{1,2}, Christine Schedel¹, Marcus Scheele^{1,2,}*

¹ Institute of Physical and Theoretical Chemistry, University of Tübingen, Auf der
Morgenstelle 18, 72076 Tübingen, Germany

² LISA+, University of Tübingen, Auf der Morgenstelle 15, 72076 Tübingen, Germany

Light microscopy images and flake height

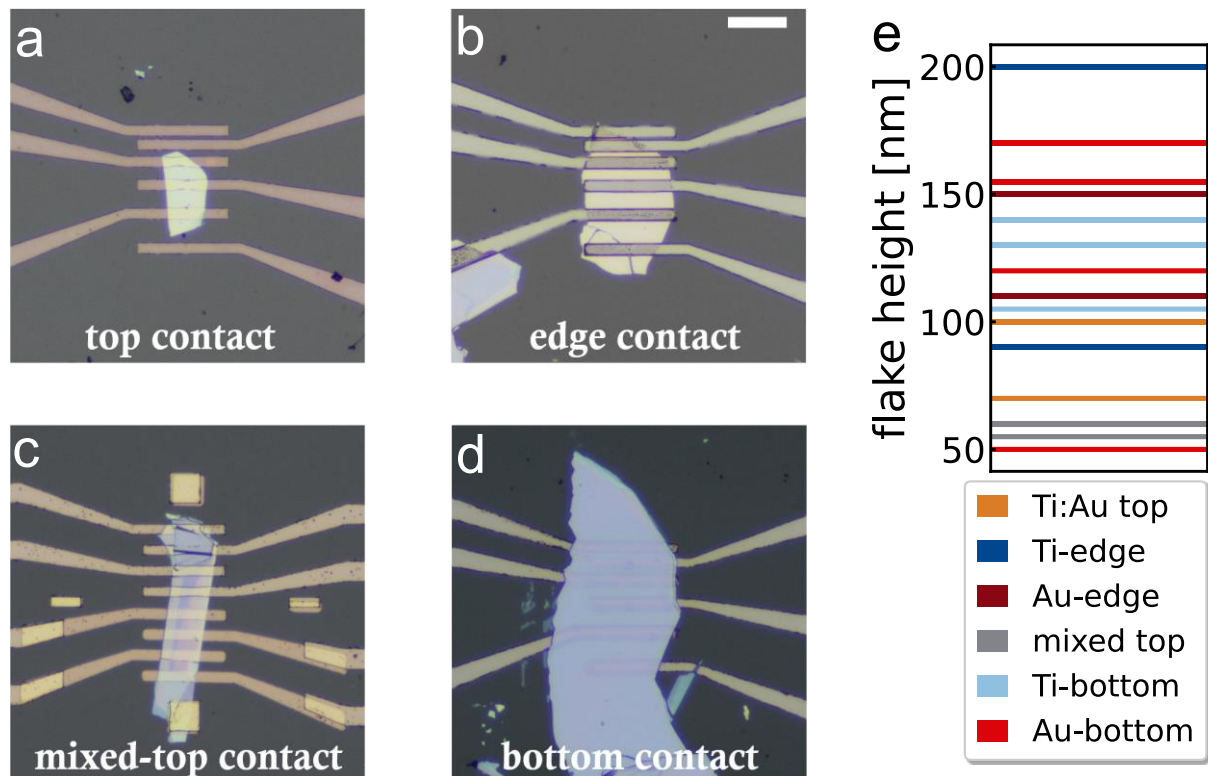


Figure S11. Light microscopy images of MoS₂ flakes with different electrode styles: a) edge contact; b) top contact; c) mixed top contact; d) bottom contact. e) Flake height for every examined flake, measured with a profilometer (*Dektak XT*). The thickness ranges from 50 nm to 200 nm. The scale bar is 50 μm .

SEM-images of an etched flake

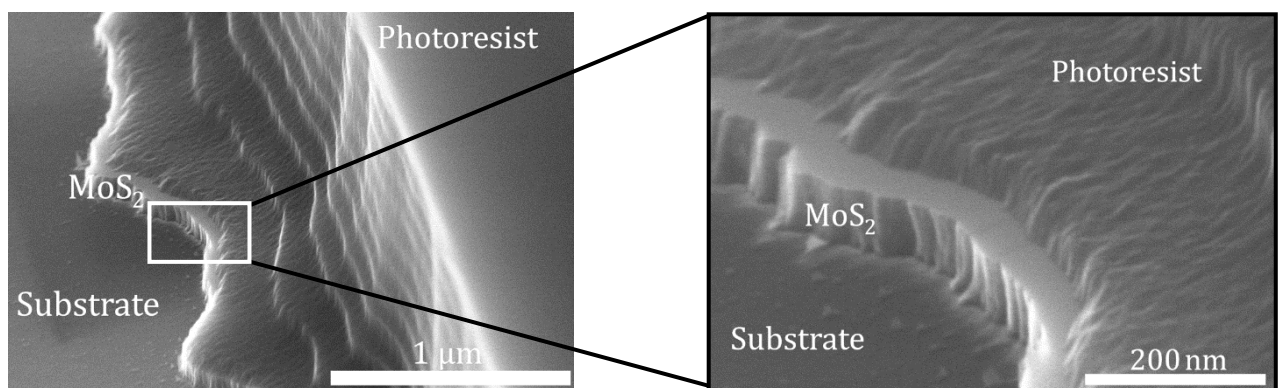


Figure S12. SEM images of an etched MoS₂ flake. a) Overview with visible resist flank, b) zoomed in image of the marked spot in a). The height of this particular flake is approximately 70 nm.

Lithographic process for fabricating edge contacts

For bottom contacts, the lithography is done prior to the exfoliation. For top contacts, the fabrication is exactly the same as in Figure SI4, only the etching part (Figure SI4c) is left out.

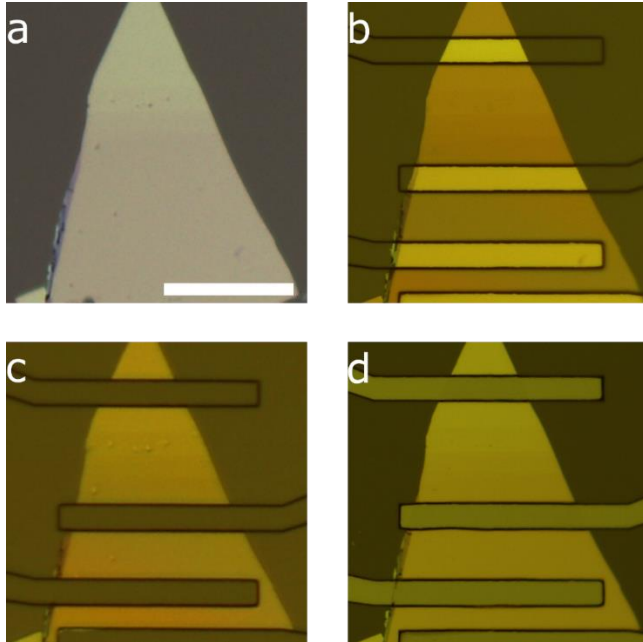


Figure SI3. Fabrication process of an edge contact: a) exfoliated flake on a glass substrate; b) patterned electrodes after photolithography and resist development; c) flake after O_2/SF_6 plasma etching; d) flake after evaporation of the electrodes. The scale bar is 50 μm .

Edge contacts are obtained by following the lithographic steps depicted in Figure SI3. The mixed top contacts are fabricated in two lithographic processes: In the first one, the upper four electrode fingers, cf. Figure SI1c, are made as well as the leads with 4 nm Ti and 20 nm Au. After lift-off, the lithography is repeated and the lower four electrodes consisting of 25 nm Au are evaporated without a wetting layer of titanium.

Persistent photocurrents in MoS₂ flakes

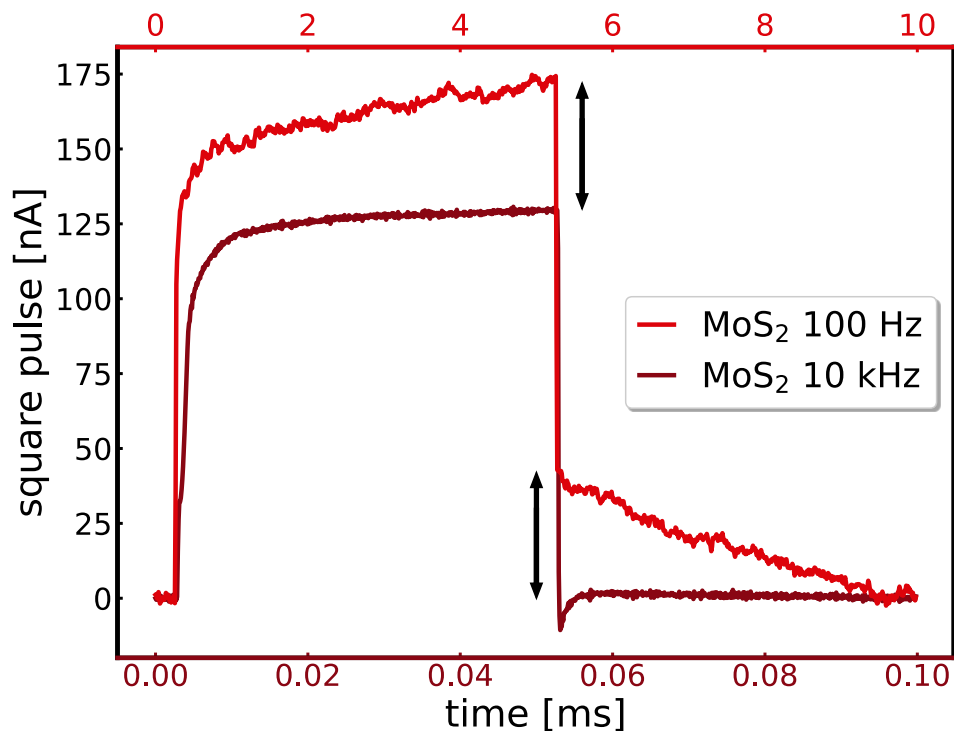


Figure SI4. 635 nm square pulse measurements of a 20 μm Au edge contact under 1 V bias. Bright red shows the measurement with a laser repetition rate of 100 Hz and dark red with 10 kHz. The two black arrows are equally long, indicating the height difference caused by the slow parts in the rise and fall time for the 100 Hz measurement.

For measurements at 100 Hz, a persistent photocurrent is sometimes observable, more pronounced for higher voltages. This can be seen in a steep increase and decrease of the rise and fall time respectively, followed by a slow and steady increase / decrease, cf. Figure SI4 bright red curve. These two effects can be attributed to the fast photoconductive and the slower photogating effect. Di Bartolomeo et al.¹ examined that the slower photogating relies on deeper traps which yield very long response times, but require a longer exposure to be filled. Thus, this behaviour can be suppressed when switching to higher repetition rates like 10 kHz, showing only the relevant photoconductive component.

I-V characteristics

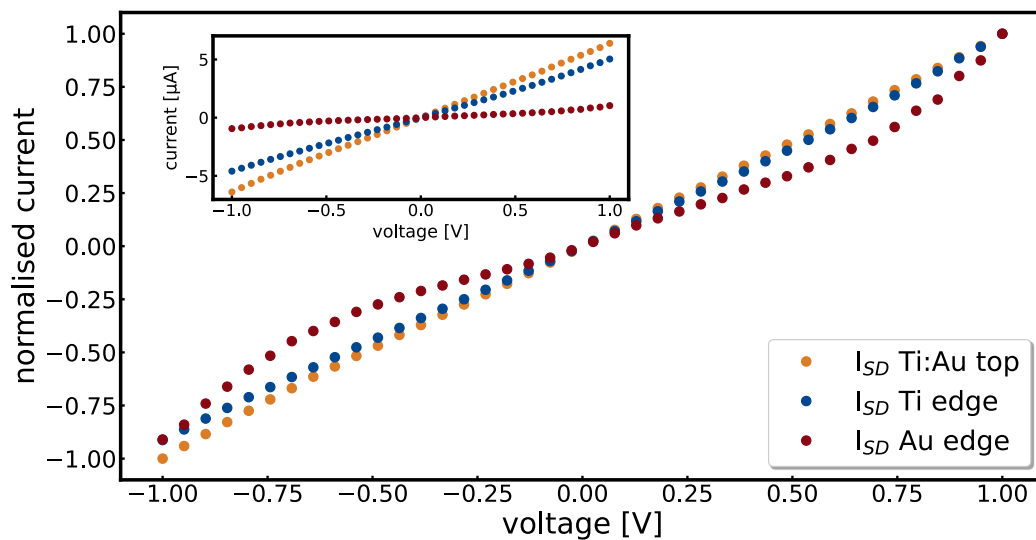


Figure SI5. Normalized I-V characteristics of a Ti:Au top (ochre), a Ti edge (blue) and a Au edge (red) contacted flake without illumination. Measurements made on 10 μm contacts from -1 to 1 V. The inset shows the absolute current values. The slope can be translated into resistances of 161 $\text{k}\Omega$, 218 $\text{k}\Omega$ and 1.46 $\text{M}\Omega$ respectively.

The I-V characteristic shows the same trend observed in literature: for a titanium contacting, either top or edge, there is an (nearly) ohmic behaviour, whereas for a gold contacting the curves tend to differ due to the higher Schottky barrier. The dark currents are generally rather high, due to the bulk MoS_2 flakes.

Band diagram of an Au top and an Au edge contact

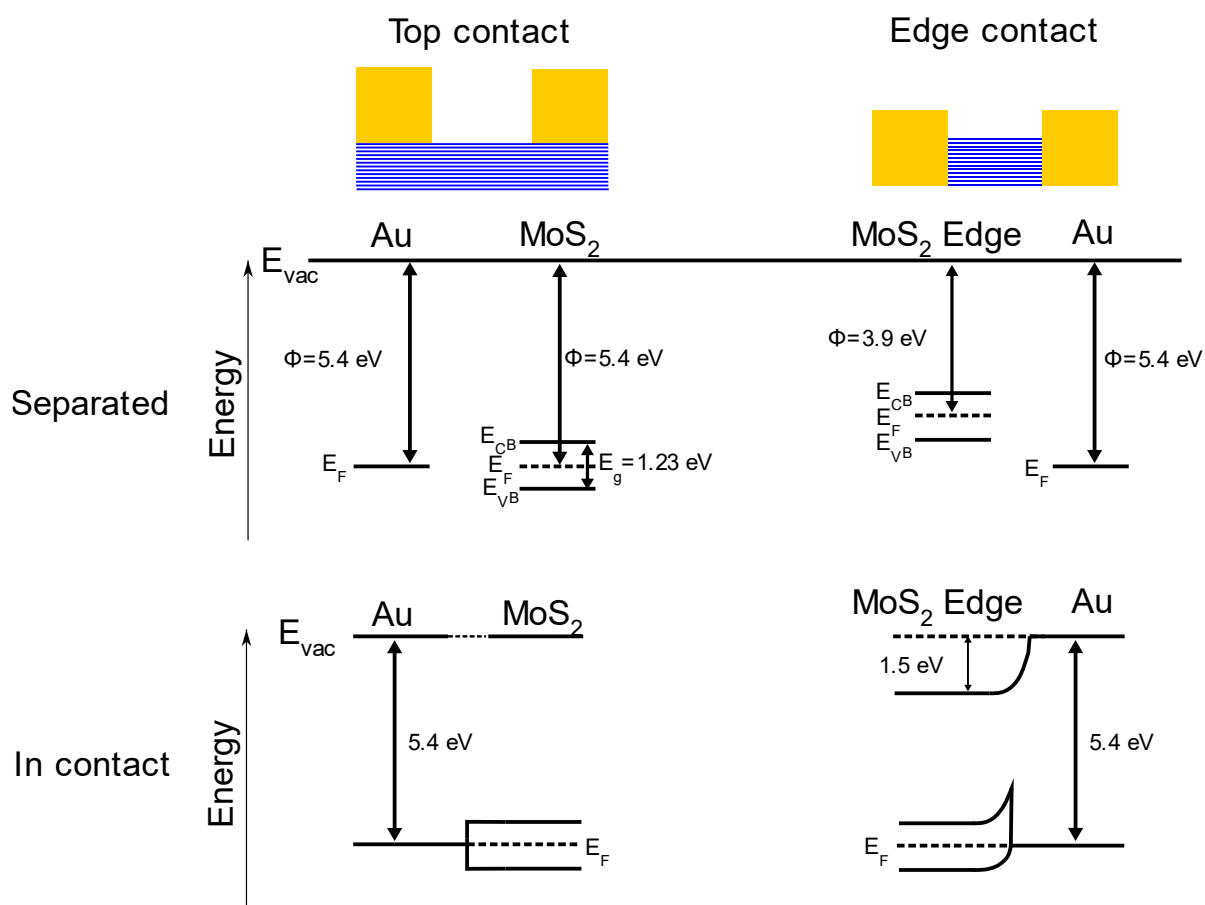


Figure SI6. Band diagrams for an idealized top contact (left) and edge contact (right). The upper half shows all the work functions extracted from literature²⁻⁵. At the bottom, an idealized model of the materials brought into contact can be seen.

The band diagram in Figure SI6 shows an idealized model of a top and an edge contact consisting of gold and MoS₂. Thereby, it is important to use the appropriate MoS₂ work function, depending on the electrode geometry. When contacting the edge, a larger Schottky barrier arises than when contacting from the top. It is important to emphasise, that those literature values may differ in reality, depending on the nature of the semiconductor (n- or p-type or intrinsic), the exact work function of Au and stress, strain, defects or any order form of imperfection in the MoS₂ flake, to name just a few examples. Additionally, metallization at the edge contact might occur, altering the band model⁶.

Rise / fall time vs channel length and voltage

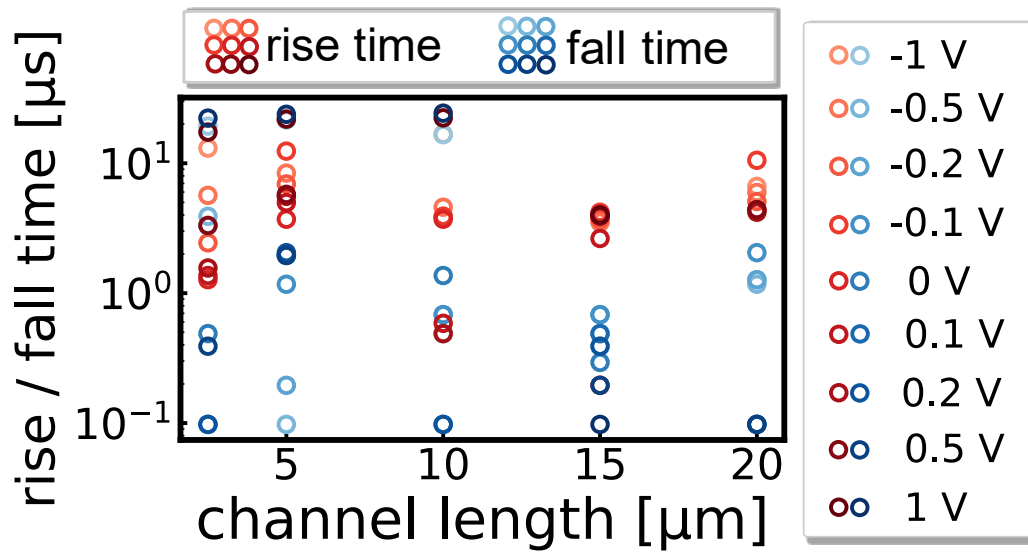


Figure SI7. Rise times (red) and fall times (blue) of 10 kHz measurements of an Au edge contact plotted vs the channel length. The different shades resemble the different biases applied.

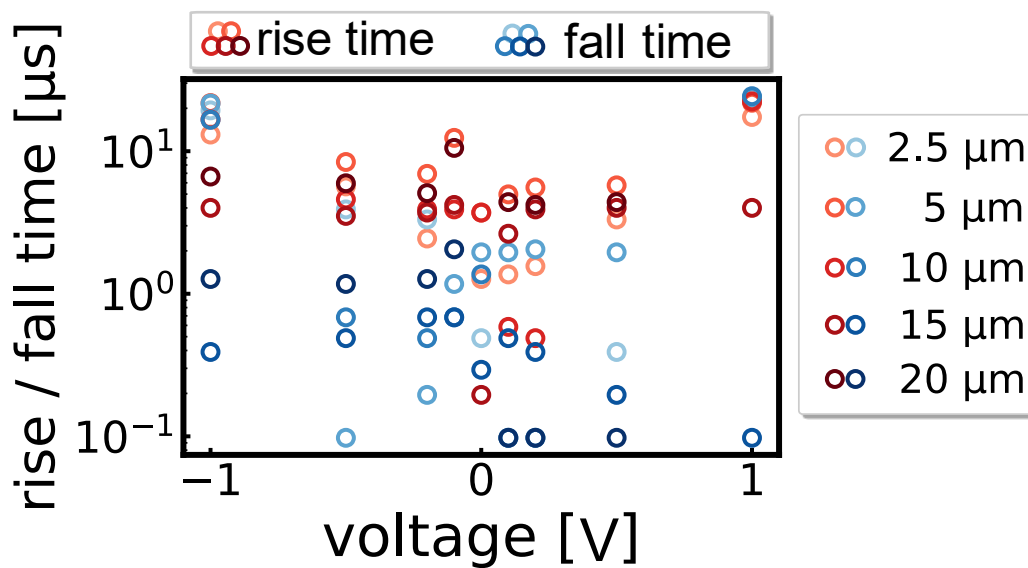


Figure SI8. Rise times (red) and fall times (blue) of 10 kHz measurements of an Au edge contact plotted vs the bias voltage. The different shades resemble the different channel lengths of the electrodes.

There is no clear trend visible towards the applied voltage or channel length. Therefore, we cannot further determine the speed limiting mechanism of the MoS₂ flakes.

Impulse response and bandwidth of the fastest device

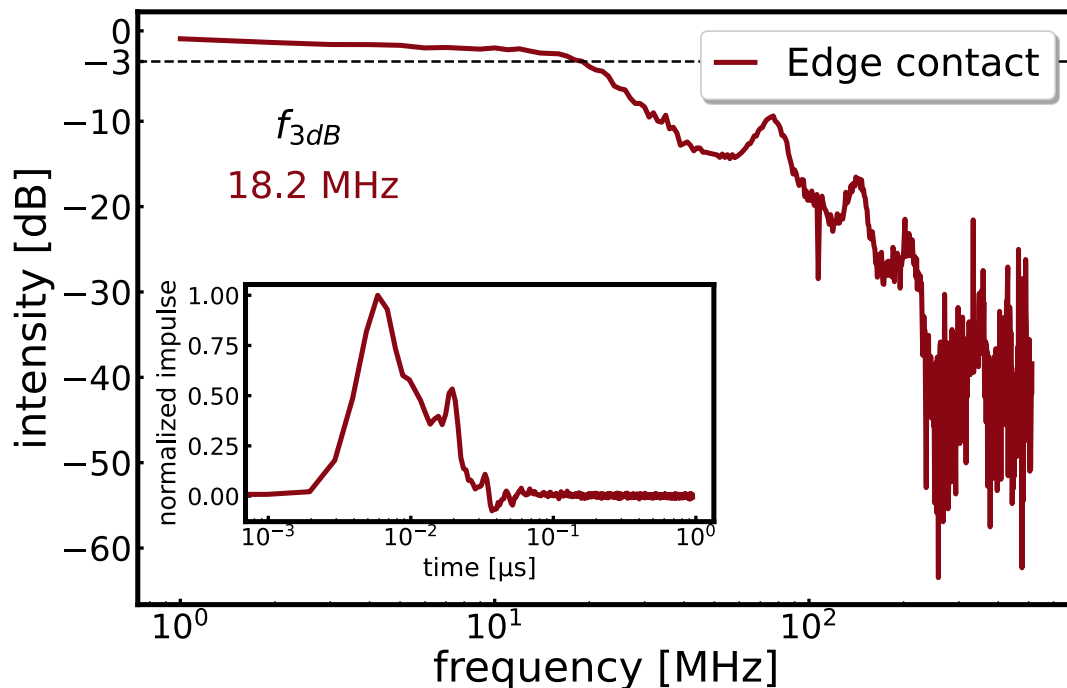


Figure SI9. Bandwidth of fastest MoS₂ photodetector fabricated. The inset shows the impulse response of a 10 μm channel with 0.5 V applied bias of an Au edge contacted device towards a 636 nm laser operated at 1 MHz repetition rate. The graph shows the Fourier transformation of the impulse response.

References

- (1) di Bartolomeo, A.; Genovese, L.; Foller, T.; Giubileo, F.; Luongo, G.; Croin, L.; Liang, S. J.; Ang, L. K.; Schleberger, M. Electrical Transport and Persistent Photoconductivity in Monolayer MoS₂ Phototransistors. *Nanotechnol.* **2017**, *28*, 214002
- (2) Asadi, M.; Kumar, B.; Behranginia, A.; Rosen, B. A.; Baskin, A.; Repnin, N.; Pisasale, D.; Phillips, P.; Zhu, W.; Haasch, R.; Klie, R. F.; Král, P.; Abiade, J.; Salehi-Khojin, A. Robust Carbon Dioxide Reduction on Molybdenum Disulphide Edges. *Nat. Comm.* **2014**, *5*.
- (3) Greulich, K.; Belser, A.; Bölke, S.; Grüninger, P.; Karstens, R.; Sättele, M. S.; Ovsyannikov, R.; Giangrisostomi, E.; Basova, T. v.; Klyamer, D.; Chassé, T.; Peisert, H. Charge Transfer from Organic Molecules to Molybdenum Disulfide: Influence of the Fluorination of Iron Phthalocyanine. *J. Phys. Chem. C* **2020**, *124*, 16990–16999.
- (4) Uda, M.; Nakamura, A.; Yamamoto, T.; Fujirnoto, Y. Work Function of Polycrystalline Ag, Au and Al. *J. Electron Spectros. Relat. Phenomena* **1998**, *91*, 643–648.
- (5) Baik, S. S.; Im, S.; Choi, H. J. Work Function Tuning in Two-Dimensional MoS₂ Field-Effect-Transistors with Graphene and Titanium Source-Drain Contacts. *Sci Rep* **2017**, *7*, 1–8.
- (6) Yang, Z.; Kim, C.; Lee, K. Y.; Lee, M.; Appalakondaiah, S.; Ra, C. H.; Watanabe, K.; Taniguchi, T.; Cho, K.; Hwang, E.; Hone, J.; Yoo, W. J. A Fermi-Level-Pinning-Free 1D Electrical Contact at the Intrinsic 2D MoS₂–Metal Junction. *Adv. Mater.* **2019**, *31*.